Monatshefte für Chemie 133, 1351–1361 (2002)

Monatshefte für Chemie
Chemical Monthly

Effect of the Preparation Method of Al–Mg–O Catalysts on the Selective Decomposition of Ethanol

Ahmed A. Abd El-Raady[1], **Nasr E. Fouad**[2], **Mohamed A. Mohamed**[1], and **Samih A. Halawy**[1,*]

[1] Chemistry Department, Faculty of Science, South Valley University, Qena 83523, Egypt
[2] Chemistry Department, Faculty of Science, Minia University, 61519 El-Minia, Egypt

Summary. Selective decomposition of ethanol was used as a test reaction at 350°C to evaluate the catalytic activity of two Al–Mg–O mixed oxides prepared by two different methods (wet impregnation and coprecipitation). The catalyst precursors were examined by TG and DTA and were calcined between 500–900°C for 5 h in air. The surface area of all catalysts was measured by N_2 sorption using the BET method. The total acidity and basicity were determined by TPD using pyridine and formic acid. The catalysts were characterized by XRD analysis. It was found that the preparation method of Al–Mg–O catalyst has a great effect on the selective decomposition of ethanol. Al–Mg–O (I) catalysts, prepared by wet impregnation, were more selective towards ethene formation during dehydration of ethanol. This is ascribed to their high total surface acidity. On the other hand, Al–Mg–O (II) catalysts, prepared by coprecipitation, were highly selective in the oxidative dehydrogenation of ethanol to yield acetaldehyde. This could be attributed to their high concentration of basic sites. In addition, the production of traces of diethyl ether was also observed (three times more for Al–Mg–O (II) than for Al–Mg–O (I)).

Keywords. Al_2O_3; Characterization; Ethanol; MgO; Selective decomposition.

Introduction

The selective decomposition of alcohols on solid catalysts is known [1, 2] to take place *via* two pathways: by dehydration, which is generally catalyzed by acidic sites, and by dehydrogenation which is initiated by basic sites or both acidic and basic sites [1, 2]. This selectivity has been used as an indicator of the acidic and basic character of the surface of solid catalysts [3–5]. The correlation between the catalytic activity during the decomposition of alcohols with one to three carbon atoms and the acidic–basic surface properties of different catalysts has been studied for different catalyst systems, *e.g.* Al–Mg–O [6, 7], Al–Ni–O [8], smectite clays [9, 10], and MgO [4]. There is great industrial interest to convert low alcohols into useful organic intermediates or products, *i.e.* ethene, diethyl ether, or acetaldehyde.

* Corresponding author. E-mail: shalawy99@yahoo.com

Ethanol serves as a feedstock for acetaldehyde production *via* oxidative dehydrogenation over pure or mixed oxide catalysts [11–14].

Surfaces of fully dehydroxylated ionic oxides can be considered as a perfect distribution of coordinatively unsaturated positively (cations) and negatively (oxides) charge centers [15]. The coordinative unsaturation of the individual centres depends upon the type of exposed faces. On the other hand, the effective charge carried by each surface centre depends primarily upon the bulk property, *i.e.* ionicity of the oxide under consideration. For Al–Mg oxide mixtures, changes in their acidic–basic surface character may also be caused by an inductive effect due to the incorporation of aluminum. Accordingly, doping a MgO lattice with Al should enhance both the *Lewis* acidity and its reactivity towards alcohol dehydration [16].

In this work we attempted to investigate the effect of the preparation method of Al–Mg–O oxide mixtures on their surface properties and hence their catalytic reactivity during the selective decomposition of ethanol.

Results and Discussion

Thermal analysis

TG and DTA curves of the Al–Mg–O (I) precursor are shown in Fig. 1a. The TG curve exhibits four overlapping mass loss steps between 38 and 296°C with a total mass loss of 19.7%. These steps correspond to the stepwise dehydration of

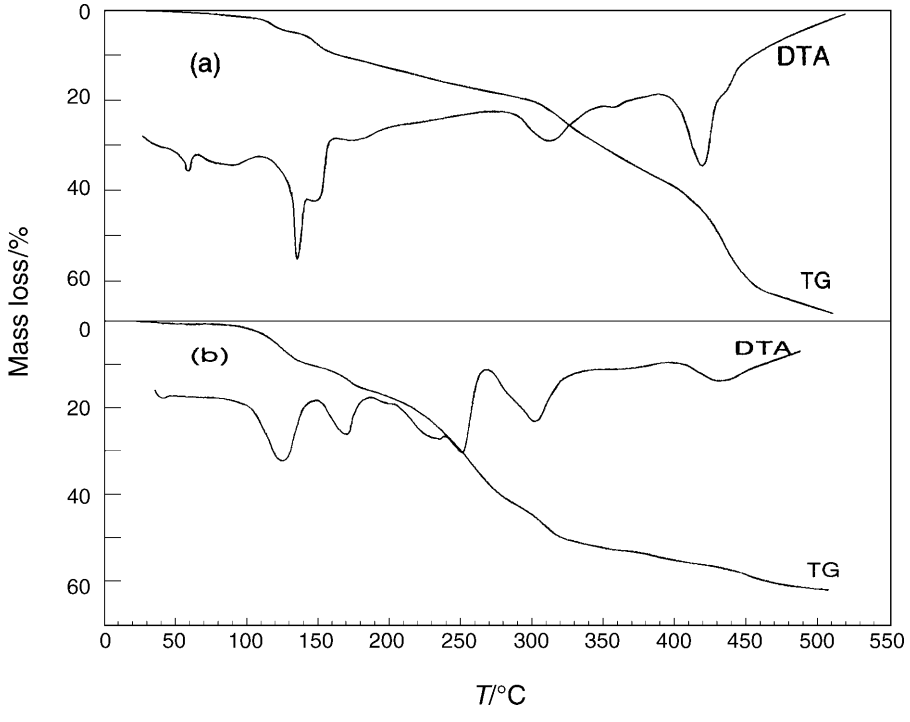

Fig. 1. TG and DTA curves of the thermal decomposition of (a) Al–Mg–O (I) and (b) Al–Mg–O (II) precursors ($10°C \cdot min^{-1}$, a dynamic N_2 atmosphere ($40\,cm^3 \cdot min^{-1}$))

aluminum nitrate [22]. Two consecutive steps follow in the temperature range of 296–470°C. The first one (at 296–418°C) is due to the decomposition of $Al(NO_3)_3$ together with the initial decomposition of $MgCO_3$ present in this mixture [23], the second is attributed to the main decomposition of $MgCO_3$. The mass loss values accompanied with these two steps are 20.2 and 26.9%, respectively. The total mass loss of Al–Mg–O (I) at 500°C equals 66.8%. The DTA curve of this sample displays a group of endothermic peaks at 57, 89, 134, 146, and 175°C due to the dehydration of $Al(NO_3)_3 \cdot 9H_2O$, followed by an endothermic peak at 310°C attributed to the decomposition of the anhydrous $Al(NO_3)_3$. The three endothermic peaks located at 353 (weak), 418 (sharp), and at 435°C (shoulder) are ascribed to the decomposition of $MgCO_3$ [23] and the formation of MgO. The TG curve of Al–Mg–O (II) (Fig. 1b) exhibits five mass loss steps in the temperature range of 50–319°C associated with a total mass loss of 49.2%. The DTA curve of Al–Mg–O (II) (Fig. 1b) also showed five endothermic peaks at $T_{max} = 123$, 169, 232, 249, and 299°C corresponding to the above mentioned five mass loss steps due to the dehydration and dehydroxylation of aluminum hydroxide. The TG curve shows another mass loss step between 320 and 490°C associated with a mass loss of 11.9%. This step is attributed to the decomposition of $Mg(OH)_2$. The DTA curve shows an endothermic peak at 432°C corresponding to the last mass loss step for the decomposition of $Mg(OH)_2$ [24].

From the thermal analysis results it can be concluded that at 500°C both Al–Mg–O (I) and Al–Mg–O (II) are completely decomposed and the corresponding oxides of Al_2O_3 and MgO are produced.

X-Ray diffraction analysis

XRD patterns of the different samples of Al–Mg–O (I) calcined at different temperatures are shown in Fig. 2. All samples are composed of MgO (ICDD 4-829) and the spinel $MgAl_2O_4$ (ICDD 21-1152) as major components. Three minor phases of alumina (γ-Al_2O_3 (ICDD 29-63), δ-Al_2O_3 (ICDD 4-877), and corundum (α-Al_2O_3 (ICDD 10-173)) are observed for samples calcined between 700 and 900°C. Figure 3 displays the XRD patterns of Al–Mg–O (II) calcined at different temperatures. Again, the main components of these mixtures are MgO and the spinel $MgAl_2O_4$. In addition, at 500 and 600°C there is a diffraction line of high intensity at $d = 2.004$ Å due to the formation of γ-Al_2O_3. At higher calcination temperatures (*i.e.* 700–900°C), another diffraction line appeared at $d = 1.649$ Å belonging to α-Al_2O_3. From the XRD results it can be noticed that the spinel $MgAl_2O_4$ and MgO have been formed in these mixtures during the two preparation methods.

Surface area and density of acidic and basic sites

All calcined catalysts possessed S_{BET} values between 35.5 and 142 $m^2 \cdot g^{-1}$ (Table 1). As the calcination temperature increases, the surface area gradually decreases. The basic sites density of the catalyst samples were higher than the acidic sites. Al–Mg–O (II) derived catalysts calcined at 500–900°C were more basic than the corresponding catalysts produced from Al–Mg–O (I). This is in

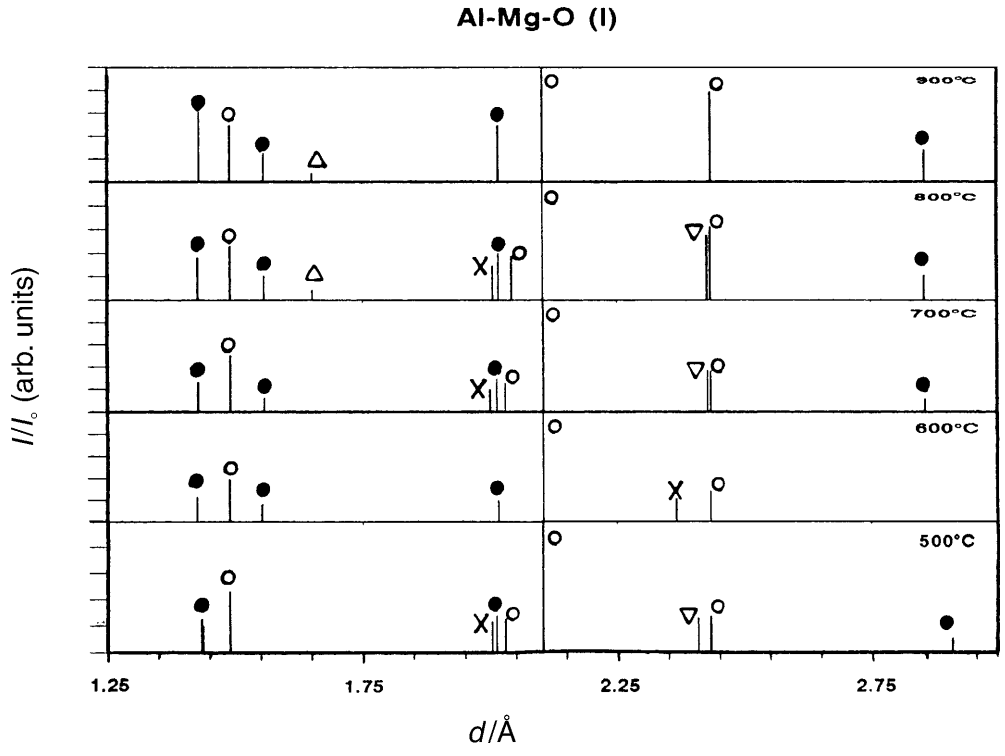

Fig. 2. XRD patterns of Al–Mg–O (I) calcined at the indicated temperatures for 5 h; ○: MgO, ●: $MgAl_2O_4$, ×: γ-Al_2O_3, △: α-Al_2O_3, ▽: δ-Al_2O_3

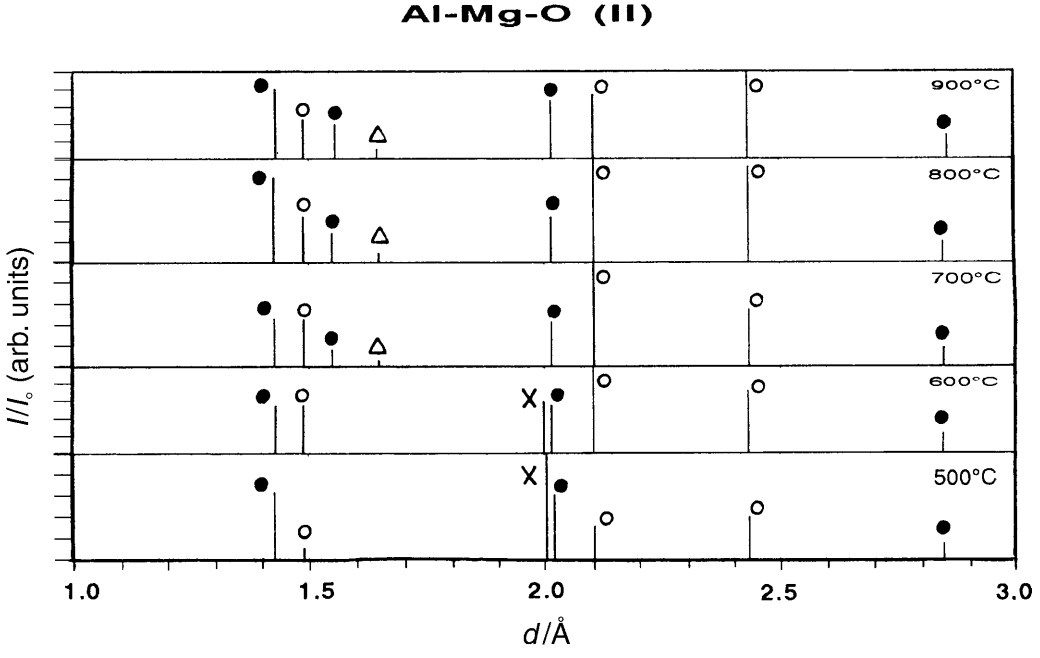

Fig. 3. XRD patterns of Al–Mg–O (II) calcined at the indicated temperatures for 5 h; ○: MgO, ●: $MgAl_2O_4$, ×: γ-Al_2O_3, △: α-Al_2O_3

Table 1. S_{BET}, acidity–basicity, and kinetic parameters of the selective decomposition of ethanol over Al–Mg–O (I) and Al–Mg–O (II) calcined at different temperatures for 5 h

	Al–Mg–O (I)					Al–Mg–O (II)				
	500°C	600°C	700°C	800°C	900°C	500°C	600°C	700°C	800°C	900°C
S_{BET} ($m^2 \cdot g^{-1}$)	142.0	136.7	100.1	73.1	45.1	113.1	109.9	72.7	52.6	35.5
Acidity[a] ($\Psi \times 10^{21}$)	21.4	9.9	8.2	6.8	5.3	18.6	8.3	6.4	5.3	4.4
Basicity[a] ($\Phi \times 10^{21}$)	43.0	51.0	66.0	72.0	97.0	49.0	52.0	68.0	89.0	124.0
Ψ/Φ	0.498	0.194	0.124	0.094	0.055	0.380	0.160	0.094	0.059	0.035
Conversion	12.1	9.8	9.9	7.5	5.5	13.9	10.0	7.5	6.5	5.9
R^b_{total}	129.5	104.9	105.9	80.3	58.9	148.7	107.0	80.3	69.6	63.1
R^b_E	68.8	51.5	50.4	33.1	17.7	60.4	42.8	23.4	15.8	9.9
R^b_A	53.0	47.7	49.3	46.4	41.2	65.7	49.9	50.5	51.4	52.7
R^b_{DEE}	7.7	5.7	6.1	0.8	0.0	22.6	14.3	6.4	2.4	0.5

[a] Sites per m^2 of catalyst; [b] $mmol \cdot h^{-1} \cdot m^{-2}_{cat}$

contrast with the trend in the acidic character of both catalyst samples. As the calcination temperature increased from 500 to 900°C, the density of the acidic sites decreased in both catalysts. This can be due to the interaction of alumina which contains both *Lewis* and *Brönsted* acidic sites [24] with MgO to give $MgAl_2O_4$ as concluded from the XRD analysis. This is confirmed by the increasing intensity of the diffraction lines at $d = 1.430$, 1.557, 2.017, and 2.855 Å of $MgAl_2O_4$ (ICDD card 21-1152) with increasing calcination temperature (Figs. 2 and 3). In addition, according to XRD analysis the main constituents of these samples were $MgAl_2O_4$ and the fairly basic oxide MgO [25, 26]. Therefore, the ratio Ψ/Φ, *i.e.* the concentration ratio of the acidic relative to the basic sites, is diminished steadily as the temperature increases from 500 to 900°C.

Catalytic decomposition of ethanol

It is well known [1] that basic catalysts (as pure or mixed oxides) promote alcohol dehydrogenation, whereas acidic catalysts initiate the dehydration reaction of alcohols. Therefore, the dehydration activity of these catalysts increases with increasing density of acidic sites [10]. Ethene and acetaldehyde were found to be the major products of ethanol decomposition at 350°C over the two catalyst samples calcined at different temperatures. In addition, diethyl ether was produced as a minor product. Figure 4 represents the effect of calcination temperature on the acid site density (Ψ), the selectivity of ethene (S_E), and the selectivity of diethyl ether (S_{DEE}) over the catalysts under investigation. The values of both S_E and S_{DEE} correlated with Ψ for all catalysts. S_E, S_{DEE}, and Ψ decrease with increasing calcination temperature. In the case of Al–Mg–O (I) at 500°C, S_E (I) was calculated to be 53.1%; it decreased to 47.6% for the catalyst calcined at 700°C. Afterwards, it decreased sharply to 30% over Al–Mg–O (I) catalyst calcined at 900°C. The surface acidity Ψ (I) of the catalysts seems to behave similarly as S_E (I). Catalysts

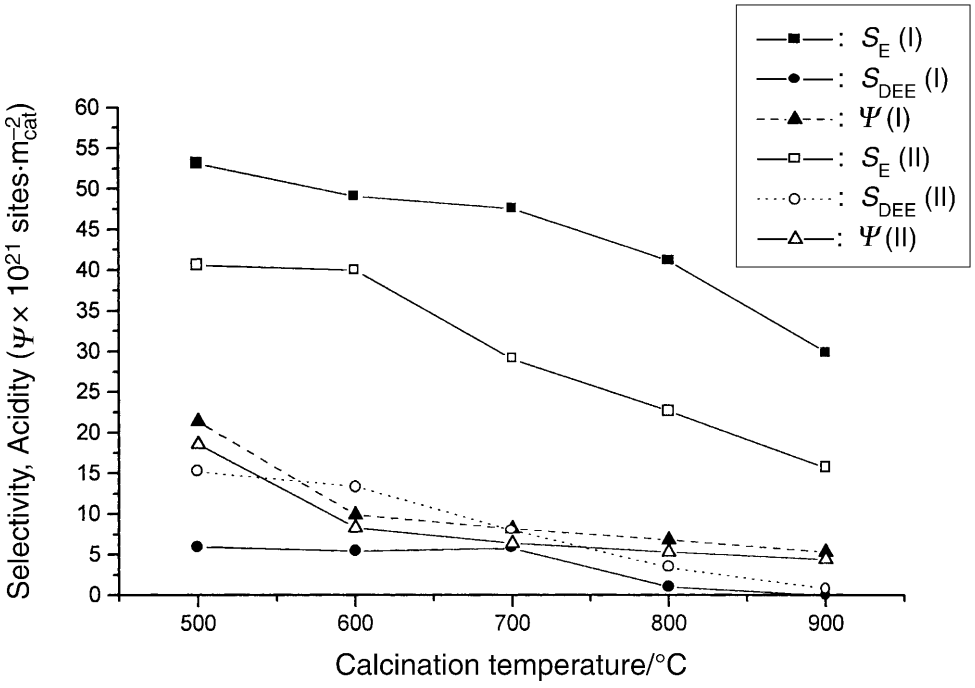

Fig. 4. Selectivities of ethene and diethyl ether and surface acidity as a function of calcination temperature of Al–Mg–O catalysts during the selective decomposition of ethanol at 350°C

derived from Al–Mg–O (I) were always more selective towards ethene formation than those originating from Al–Mg–O (II). This is due to their higher number of acidic surface sites as shown in Table 1. On the other hand, the appreciable values of S_{DEE} over catalysts calcined at 500 and 600°C become negligible over catalysts calcined at higher temperatures, *i.e.* 800 and 900°C. According to the mechanism of ethanol dehydration [28–30] over oxidic catalysts, the main step consists of the formation of the surface ethoxide ($C_2H_5O^-_{(s)}$) intermediate on the acid sites of the catalysts as follows:

$$C_2H_5OH + OH^- \rightarrow C_2H_5O^-_{(s)} + H_2O$$

This intermediate can either react with another ethanol molecule to form diethyl ether, or undergo decomposition to give ethene:

$$C_2H_5OH + C_2H_5O^-_{(s)} \rightarrow (C_2H_5)_2O + OH^-_{(s)} \text{ or } C_2H_5O^-_{(s)} \rightarrow C_2H_4 + OH^-_{(s)}$$

Therefore, the formation of the ethoxide intermediate depends mainly on the concentration of *Brönsted* acid sites (Al–OH) on the catalyst surface [19]. It is worth noting that the values of R_{DEE} (the rate of formation of diethyl ether) over catalysts of type Al–Mg–O (II) were greater than those of Al–Mg–O (I) catalysts (Table 1). This may be attributed to the presence of strongly acidic tetrahedral Al^{3+} cations [9] in catalysts of the Al–Mg–O (II) type prepared by the coprecipitation method, whereas catalysts of Al–Mg–O (I), prepared by the impregnation method, contain different types of very weak *Lewis* acid sites such as coordinatively unsaturated Al^{3+} and Mg^{2+} cations [9].

The effect of calcination temperature on the values of S_A (selectivity of acetaldehyde formation) as well as Φ (catalyst surface basicity) is shown in Fig. 5. S_A

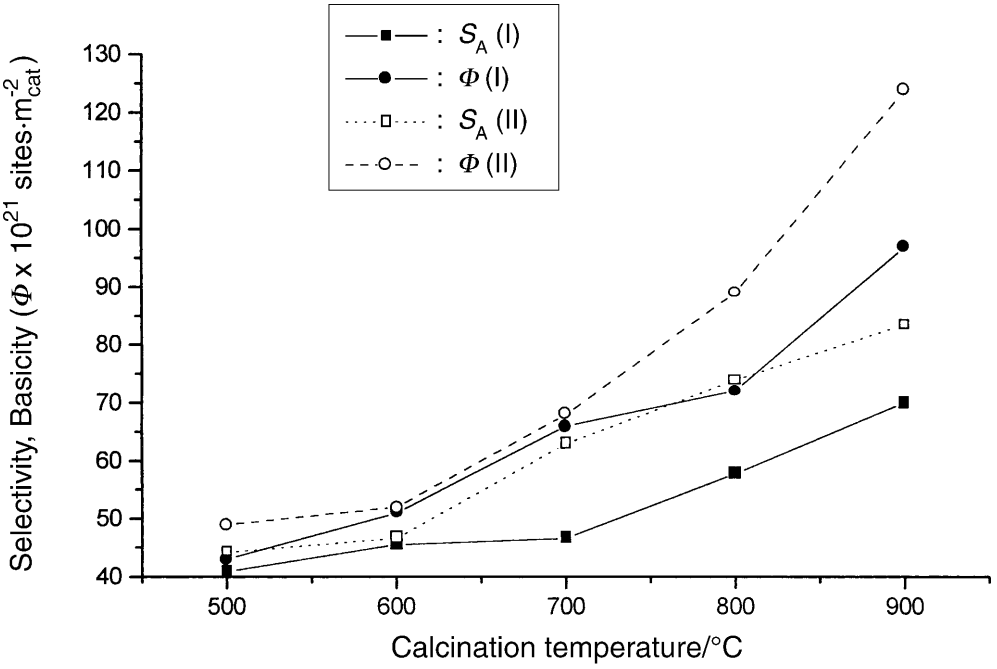

Fig. 5. Selectivity of acetaldehyde and surface basicity as a function of the calcination temperature of Al–Mg–O catalysts during the selective decomposition of ethanol at 350°C

increases with increasing calcination temperature from 500 up to 900°C. Similarly, the surface basicity of all catalysts has the same trend as S_A. Figure 5 and Table 1 show Al–Mg–O (II) catalysts to be more basic than the corresponding catalysts of the Al–Mg–O (I) type. The basic sites concentration, Φ, at 500°C for Al–Mg–O (II) is 49×10^{21} sites/m^2_{cat} and increases to a value of 124×10^{21} sites/m^2_{cat} at 900°C. On the other hand, the corresponding value of S_A (II) was 44.2% for the catalyst calcined at 500°C and steadily increased to 83.5% for Al–Mg–O (II) calcined at 900°C. Catalysts prepared from Al–Mg–O (I) were less selective towards acetaldehyde formation, especially at higher calcination temperatures ($\geq$ 700°C). S_A (I) for Al–Mg–O (I) catalysts calcined at 700, 800, and 900°C were 46.6, 57.8, and 70%, respectively. The formation of acetaldehyde by oxidative dehydrogenation of ethanol depends mainly on a reaction producing negatively charged oxide surfaces. After the adsorption of ethanol, the O–H bond will dissociate to give ethoxide and a proton as follows:

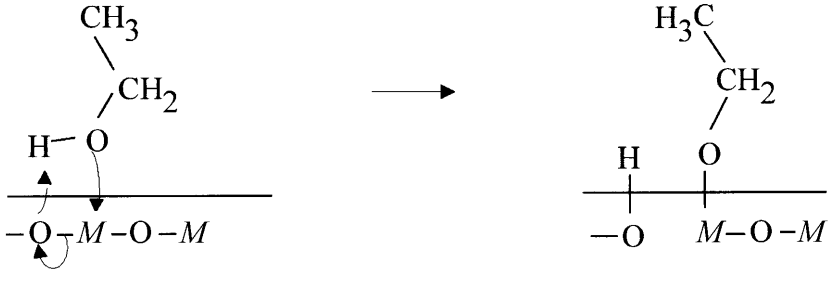

Adsorption of ethanol molecule Surface ethoxide formation

The ethoxide undergoes dehydrogenation associated with subsequent electron donation to the cation, thus yielding acetaldehyde [14]:

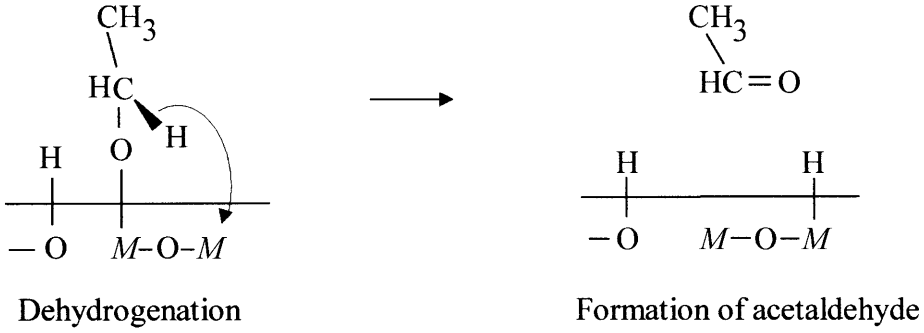

The catalyst surfaces promoting the oxidative dehydrogenation reactions are basic in character. Therefore, the more basic the catalyst surface, the higher the selectivity towards acetaldehyde formation.

It is clear from Figs. 4 and 5 that the catalysts calcined at 500°C were the most active. Consequently, Fig. 6 displays a comparison between these two most active catalysts (Al–Mg–O (I), 500°C and Al–Mg–O (II), 500°C), showing that increasing the reaction temperature from 340 to 380°C significantly improves the total conversion and the rate of formation of ethene, diethyl ether, and acetaldehyde. The conversion rate of ethanol over Al–Mg–O (II), 500°C was always higher than that over Al–Mg–O (I), 500°C and increased with the reaction temperature. At low

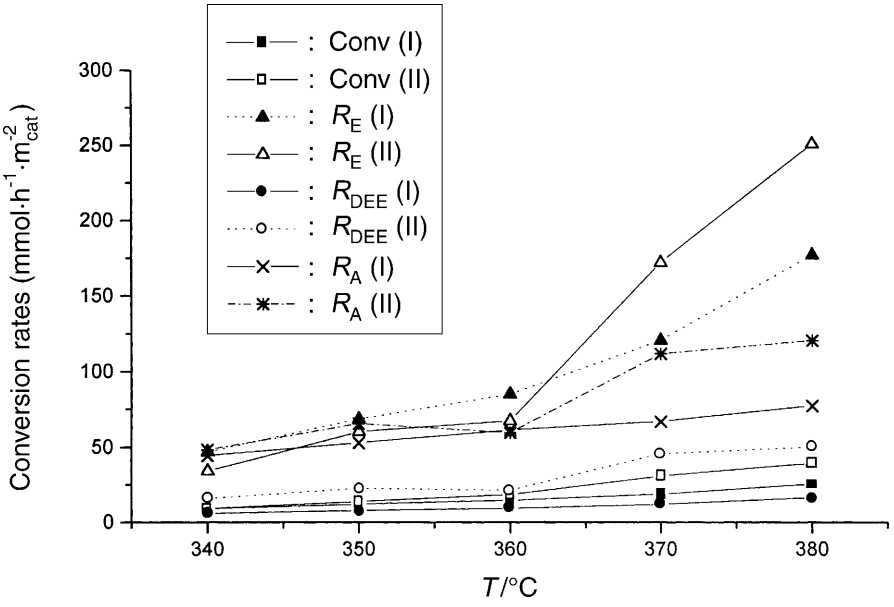

Fig. 6. Conversion and rate of product formation (ethene, diethyl ether, and acetaldehyde) as a function of the reaction temperature of the selective decomposition of ethanol over Al–Mg–O (I), 500°C and Al–Mg–O (II), 500°C

temperatures, *i.e.* below 360°C, R_E (rate of ethene formation) over Al–Mg–O (I), 500°C was greater than that over Al–Mg–O (II), 500°C. Increasing of the reaction temperature (>360°C) resulted in a significant increase of R_E over Al–Mg–O (II), 500°C, reaching a maximum at 380°C (Fig. 6). Values of R_{DEE} (rate of diethyl ether formation) over Al–Mg–O (II), 500°C were about three times greater than R_{DEE} over Al–Mg–O (I), 500°C. This could be attributed to the active acidic centres resulting from high reaction temperature and reaches its maximum activity towards dehydration reaction of ethanol over Al–Mg–O (II), 500°C. On the other hand, the values of R_A (II) (rate of acetaldehyde formation) over Al–Mg–O (II), 500°C were higher than the corresponding values over Al–Mg–O (I), 500°C at any reaction temperature except for 360°C. This could also be attributed to the high concentration of basic sites over Al–Mg–O (II), 500°C (Table 1). The basic sites became more active with increasing reaction temperature: where R_A at 370 and 380°C were 112.1 and 120.9 $\text{mmol} \cdot \text{h}^{-1} \cdot \text{m}_{\text{cat}}^{-2}$, respectively.

Conclusions

(*i*) The coprecipitation method is shown to be superior to the wet impregnation method, where the mixed hydroxides of aluminum and magnesium decompose easily to give the spinel $MgAl_2O_4$. In addition, the intensity of the XRD peaks at $d = 1.430$ and 2.017 Å becomes more intense in case of Al–Mg–O (II) compared to Al–Mg–O (I).

(*ii*) Catalysts derived from Al–Mg–O (II) calcined between 500–900°C possess a significant total surface basicity higher than that of the corresponding Al–Mg–O (I) catalysts. The surface basicity increases with increasing calcination temperature from 500 to 900°C. Catalysts of Al–Mg–O (II) were more reactive towards acetaldehyde formation.

(*iii*) Catalysts derived from Al–Mg–O (I) prepared by the wet impregnation method were found to be superior for the conversion of ethanol to ethene and diethyl ether. They showed a higher surface area S_{BET} and a higher total acidity than Al–Mg–O (II) catalysts.

(*iv*) The catalytic activity of both Al–Mg–O (I) and Al–Mg–O (II) during the decomposition of ethanol depends on their surface area (S_{BET}). Values of conversion and R_{total} (total rate of removal of ethanol) were found to decrease constantly.

(*v*) The ratio of total acidity to total basicity (Ψ/Φ) was shown to decrease with increasing calcination temperature for both groups of catalysts.

Experimental

Preparation of catalyst samples

Two samples of Al_2O_3–MgO containing 50% (w/w) of each oxide were prepared using two different methods:

(*i*) Wet impregnation method: 183 g of $Al(NO_3)_3 \cdot 9H_2O$ (BDH, England) were dissolved in a sufficient amount of deionized H_2O. Then, 52.3 g of $MgCO_3$ (Prolabo, France) were suspended in the former solution with continued stirring. The homogeneous paste was evaporated over a water bath

to complete dryness and finally dried at 120°C overnight in an oven. This mixture was calcined for 5 h in air at different temperatures (*ca.* 500, 600, 700, 800, and 900°C). This sample is referred to as Al–Mg–O (I).

(*ii*) Coprecipitation method: 65.4 g of anhydrous $AlCl_3$ and 126.1 g of $MgCl_2 \cdot 6H_2O$ (BDH, England) were dissolved in 200 cm^3 of deionized H_2O in a 2 dm^3 beaker under stirring with a magnetic stirrer at room temperature. NH_4OH (0.5 *M*) was added dropwise with constant stirring until the *pH* of the mixture reached 8.5. The mixture was then filtered off and washed several times with deionized water until the filtrate was free of chloride ions. The precipitate was evaporated and dried as mentioned above; then it was calcined at the same conditions as described for Al–Mg–O (I). The product thus obtained is referred to as Al–Mg–O (II).

Characterization

The two mixtures Al–Mg–O (I) and Al–Mg–O (II), dried at 120°C, were subjected to thermogravimetry (TG) and differential thermal analysis (DTA) using a Shimadzu stand-alone thermal analyzer (TG-50H and DTA-50, Japan). TG and DTA analyses were carried out at the following experimental conditions: heating rate = 10°C $\cdot$ min^{-1}, dynamic atmosphere of N_2 (40 $cm^3 \cdot min^{-1}$), constant sample weights (10–15 mg). α-Al_2O_3 (Shimadzu) was the thermally inert reference material for DTA experiments. X-Ray powder diffraction analysis was carried out with an X-ray diffractometer model D5000 (Siemens, Germany) with Ni-filtered CuK_α radiation ($\lambda = 1.5418$ Å, 40 kV, 30 mA). Diffractograms were recorded in the 2θ range between 30–70° with 0.02°/s at ambient temperature. An on-line data acquisition and handling system facilitated automatic JCPDS library search and match (Diffrac software, Siemens) for phase identification purposes. Specific surface areas were calculated using the BET method from the nitrogen adsorption isotherms measured on the calcined samples at liquid N_2 temperature (*ca.* -196°C) using an automatic ASAP 2010 Sorptometer of Micromeretics (USA).

The total basic and acidic sites of the catalysts were determined by temperature-programmed desorption (TPD) of formic acid and pyridine, respectively [17, 18]. The population of both acid surface sites Ψ and basic sites Φ were estimated as described previously [19].

Catalytic activity measurements

The catalytic decomposition of EtOH was performed in a fixed bed reactor by a continuous flow method under atmospheric pressure. EtOH was fed from a saturator at 3°C, and the total feed flow rate of 120 cm^3 (STP) min^{-1} was composed of 2.2 cm^3 (STP) C_2H_5OH and 117.8 cm^3 (STP) min^{-1} dry N_2. A catalyst mass of 0.3 g was stabilized in a pyrex glass reactor for 1 h at 200°C before measurements in a stream of N_2. The reactor effluent was analyzed using a gas chromatograph (Shimadzu GC-14A) equipped with a data processor (Shimadzu chromatopac C-R4AD, Japan). A flame ionization detector (FID) and a stainless steel column (PEG 20M 20% on chromosorb W, 60/80 mesh, 3 m×3 mm) at 120°C were used to identify EtOH and the decomposition products. Conversion and selectivity of each product during the decomposition of C_2H_5OH were expressed as mol% of all decomposition products per mol% of supplied $C_2H_5OH \times 100$ and mol% of particular product per mol% of all decomposition products×100, respectively. The total reaction rate can be expressed as $R_{total} = (\%\text{conversion}/100)/(W/F)$, where W is the catalyst weight (g) and F is the total flow rate of C_2H_5OH (STP) ($cm^3 \cdot h^{-1}$); the rate of formation of each product is $R_{total} \times$selectivity of that product [20, 21].

References

[1] Nakajima T, Nameta H, Miishima S, Matsuzaki I, Tanabe K (1994) J Mater Chem **3**: 853
[2] Ai M, Suzuki S (1974) Bull Jpn Petrol Inst **16**: 118
[3] Hao Y, Tao L, Zheng L (1994) Appl Catal A **115**: 219

[4] Wang JA, Bokhimi X, Novaro O, López T, Gomez R (1999) J Mol Catal A **145**: 291
[5] Yang J-I, Lee D-W, Lee J-H, Hyun JC, Lee K-Y (2000) Appl Catal A **194–195**: 123
[6] Gervasini A, Fenyvesi J, Auroux A (1997) Catal Lett **43**: 219
[7] Fishel CT, Davis RJ (1994) Catal Lett **25**: 87
[8] Gervasini A, Bellussi G, Fenyvesi J, Auroux A (1995) J Phys Chem **99**: 5117
[9] Trombetta M, Busca G, Lenarda M, Storaro L, Ganzerla R, Piovesan L, Lopez AJ, Alcantra-Rodrìguez M, Rodrìguez-Castellón E (2000) Appl Catal A **193**: 55
[10] Raimondo M, De Stefanis A, Perez G, Tomlinson AAG (1998) Appl Catal A **171**: 85
[11] Yee A, Morrison S, Idriss H (1999) J Catal **186**: 279
[12] Zhou H, Wang JY, Chen X, O'Young C-L, Suib SL (1998) Microporous Mesoporous Mater **21**: 315
[13] Zhang W, Desikan A, Oyama T (1995) J Phys Chem **99**: 14468
[14] Halawy SA, Mohamed MA (1995) J Mol Catal A **98**: 63
[15] Zecchina A, Lamberti C, Bordiga S (1998) Catal Today **41**: 169
[16] Tanabe K, Sumiyoshi T, Shibata K, Kiyoura T, Kitagawa J (1974) J Bull Chem Soc Jpn **74**: 1064
[17] Makarova MA, Paukshtis EA, Thomas JM, Williams C, Zamaraev KI (1994) J Catal **149**: 36
[18] Halawy SA, Al-Shihry SS, Mohamed MA (1997) Catal Lett **48**: 247
[19] El-Katatny EA, Halawy SA, Mohamed MA, Zaki MI (2000) Appl Catal A **199**: 83
[20] Bond GC, Halawy SA, Abd El-Salaam KM, Hassan EA, Ragih HM (1994) J Chem Technol Biotechnol **59**: 181
[21] Halawy SA, Mohamed MA, Abd El-Hafez SF (1994) J Mol Catal **94**: 191
[22] Mu J, Perlmutter DD (1982) Thermochim Acta **56**: 253
[23] Maitra AM (1993) Appl Catal A **104**: 11
[24] Mackenzie RC (1970) Differential Thermal Analysis, vol 1. Academic Press, London, p 247
[25] Kiviat FE, Petrakis L (1973) J Phys Chem **77**: 1232
[26] Bezouhanova CP, Al-Zihari MA (1991) Catal Lett **11**: 245
[27] Qi C, Bai T, An L (1995) React Kinet Catal Lett **54**: 131
[28] Topchieva KV, Yun-Pin K, Smirnova IV (1957) Adv Catal **9**: 799
[29] Hussein GAM, Sheppard N, Zaki MI, Fahim RB (1991) J Chem Soc Faraday Trans **87**: 2661
[30] Idriss H, Seebauer EG (2000) J Mol Catal A **152**: 201

Received October 12, 2001. Accepted (revised) January 7, 2002